

## NMR study of thorium hydride ( $\text{Th}_4\text{H}_{15}$ )

K. F. Lau and R. W. Vaughan

*Division of Chemistry and Chemical Engineering, California Institute of Technology, Pasadena, California 91125*

C. B. Satterthwaite

*Department of Physics, University of Illinois, Urbana, Illinois 61808*

(Received 3 September 1976)

Two samples of thorium hydride,  $\text{Th}_4\text{H}_{15}$ , have been examined with a variety of NMR techniques. A moment analysis of the rigid-lattice line shape provides confirming evidence for the proton locations hypothesized from x-ray measurements of the thorium positions.  $T_1$  and  $T_2$  measurements above 390°K furnish activation energies for proton motion of  $16.3 \pm 1.2$  and  $18.0 \pm 3.0$  kcal/mole, respectively, while below 350°K,  $T_{1r}$  measurements indicate an activation energy of  $10.9 \pm 0.7$  kcal/mole for proton motion. This large change in activation energy over a rather narrow temperature range indicates complex, or more than a single, mechanism for proton motion within thorium hydride.  $T_1$  at room temperature and below is dominated by relaxation due to conduction electrons ( $T_1 T = 180 \pm 10^\circ\text{K sec}$ ), and by using multiple-pulse techniques to reduce the homonuclear dipolar broadening, a temperature-dependent line shift is observed. A time-temperature hysteresis was characterized in the measurements on one of the two samples and is strongly indicative of a phase change.

### INTRODUCTION

Efforts to understand the state of hydrogen in metals and metal hydrides have resulted in recent theoretical and experimental investigations.<sup>1</sup> The theoretical speculation<sup>2</sup> that metallic hydrogen might be a high-temperature superconductor, together with the experimental discovery of superconductivity in both thorium<sup>3</sup> and palladium<sup>4,5</sup> hydrides with high hydrogen concentration, has produced additional interest in these particular materials. Unlike the  $\text{PdH}_x$  system, the higher hydride of thorium  $\text{Th}_4\text{H}_{15}$  is a stoichiometric compound which has been characterized to a considerable extent,<sup>1,6-12</sup> and the purpose of the study reported here was to further characterize  $\text{Th}_4\text{H}_{15}$  with a variety of NMR techniques where information on the environment of the protons in the solid can be obtained.

Previous NMR studies on  $\text{Th}_4\text{H}_{15}$  have included: a wideline experiment to measure the line shift as well as an activation energy for proton motion from linewidth data,<sup>9</sup> a pulse experiment to obtain activation energies from  $T_1$  and  $T_2$  data,<sup>10</sup> and  $T_1$  measurements at low temperatures to obtain information on the conduction-electron properties.<sup>11</sup> These studies used polycrystalline samples, and the first wideline work<sup>9</sup> used a sample identified as  $\text{ThH}_{3.5}$ , not felt to be exactly the same composition as the samples in the latter two experiments.

For the present work, two polycrystalline samples were prepared similarly to those in which superconductivity was discovered.<sup>3</sup> They were in the form of black powders which had been sealed in glass tubes under a partial pressure of helium

after preparation. Each of the samples was determined to be within 1% of the stoichiometric composition  $\text{Th}_4\text{H}_{15 \pm 0.15}$ , and differed primarily in the pressure and temperature used in the synthesis. The sample hydrided under the lower pressure and temperature conditions, 1 atm of  $\text{H}_2$ , and a temperature cycle initiating at 800°K and dropping to 450°K before removing the  $\text{H}_2$ , will be labeled sample A, while the one hydrided under higher pressure and temperature, 1100°K and ~10,000 psi of  $\text{H}_2$ , will be labeled sample B. The sample preparation and characterization of this stoichiometric compound is apparently quite critical since the results of the present study differ significantly from the previous NMR studies,<sup>9-11</sup> and some difference was detected between the A and B samples themselves.

### EXPERIMENTAL DETAILS

The proton NMR measurements were all made at 56.4 MHz on a spectrometer which has been described previously.<sup>13</sup>  $T_1$  was measured with a  $180^\circ-t-90^\circ$  pulse sequence, while line shapes were determined from free-induction decay (FID) signals following a  $90^\circ$  pulse. The  $90^\circ$  pulse width was approximately 2  $\mu\text{sec}$ , and the dead time (the time from the middle of the pulse to the first point of the undistorted signal) was between 2.5 and 3.0  $\mu\text{sec}$ . A Carl-Purcell cycle was performed from time to time to confirm that no significant inhomogeneous broadening contributes to the  $T_2$ 's measured.  $T_{1r}$  was measured with a  $90^\circ x$  pulse followed by an attenuated  $y$  pulse whose length was varied from 10  $\mu\text{sec}$  to 40 msec.

For the multiple pulse studies an eight-pulse cycle was used, which has been discussed in detail previously,<sup>14,15</sup> and the cycle time  $t_c$ , the time required for a single eight-pulse cycle, was kept at 42  $\mu$ sec for measurements reported here.

Three related eight-pulse sequence measurements were made, one in the conventional fashion, and two in which the eight-pulse sequence was modified by introducing a phase error in the  $P_x$  pulse. This produces the additional zeroth-order Hamiltonian<sup>15</sup>

$$\bar{\mathcal{H}}_p^{(0)} = (2/t_c)(\phi_{-x} - \phi_x)I_y, \quad (1)$$

which is capable of removing from the spectra effects of chemical shift and magnetic field inhomogeneities if the magnitude of such inhomogeneities is substantially less than the magnitude of  $\bar{\mathcal{H}}_p^{(0)}$ .

Two versions of this modified eight-pulse experiment were performed, one ( $P_x - M_y$ ) involving the use of a  $P_x$  prepulse and observation of the  $y$  component of the precessing magnetization  $M_y$ , and a second ( $-M_x$ ) involving no prepulse and observation of the  $x$  component of the precessing magnetization  $M_x$ . The rigorous analysis of the effect of these two modified eight-pulse sequences is being published elsewhere,<sup>16</sup> but can be understood by recognizing that the eight-pulse spectra normally have three major contributions to the observed line shapes: a second-order dipolar, a static magnetic field inhomogeneity, and a relaxation term.<sup>14,15,17</sup> In the  $-M_x$  version of the phase-altered, eight-pulse sequence the static magnetic field inhomogeneity term has been removed, while in the  $P_x - M_y$  version, both the magnetic field inhomogeneity term and the second-order dipolar terms do not contribute to the observed line shape. Thus, one has three unknowns and three experiments and can, in principle, separately characterize each of the major contributions to the eight-pulse line shape.

The temperature range of 40–460 °K was achieved with two probes of different constructions. The probe with a temperature range of 190–460 °K used nitrogen gas as the coolant. The low-temperature probe, connected through a liquid-helium transfer line<sup>18</sup> to a liquid-helium Dewar, used helium as coolant.

For line-shift measurements with the eight-pulse cycle between 180 °K and room temperature, the reference was acetyl chloride. The frequency of this reference was measured relative to a spherical tetramethylsilane (TMS) sample at room temperature and all results are reported relative to this TMS. At a given temperature the shift of the sample was measured with respect to the reference, and the scaling factor of the eight-pulse cycle was checked at that temperature, thus cali-

brating out any small temperature-induced effects due to the electronics. At lower temperatures the reference was a single crystal of  $\text{Ca}(\text{OH})_2$  oriented in the magnetic field such that the major axis of its proton chemical shift tensor was parallel to the external field.<sup>19</sup> It is, thus, assumed that the proton chemical shift of the  $\text{Ca}(\text{OH})_2$  remained unchanged as the temperature was varied. The error limit of the reported line shift was set liberally at  $\pm 5$  ppm because susceptibility and electron conductivity of the thorium hydride sample could affect the resonance position in the eight-pulse measurement, and the sample occupied volume in which the reference indicated that some  $H_1$  field gradient existed.

## RESULTS AND DISCUSSION

### A. Rigid lattice line shapes

Figure 1 illustrates the room-temperature on-resonance FID of  $\text{Th}_4\text{H}_{15}$ , and a beat structure is clearly present. As the temperature was lowered from room temperature to 40 °K, the FID line shape remained unchanged and no difference was noted between the two samples. To determine if this line shape is consistent with the rigid-lattice

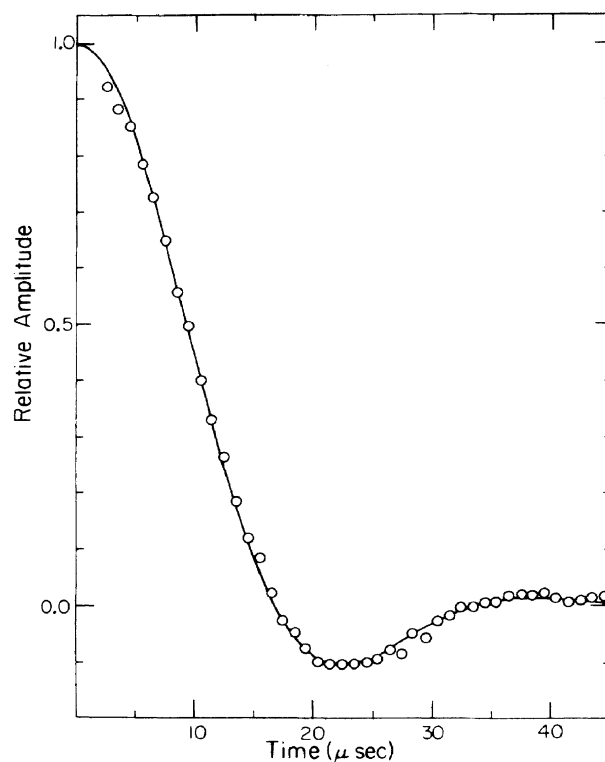


FIG. 1. Normalized free-induction-decay signal of the  $\text{Th}_4\text{H}_{15}$  powder sample ( $\circ$ ). The solid line is the analytical function  $\exp(-\frac{1}{2}at^2)(\sin bt)/bt$ , where  $a$  and  $b$  were determined from the calculated second and fourth moments for the proposed structure.

line shape for the structure of Th<sub>4</sub>H<sub>15</sub> suggested in the literature,<sup>7</sup> the second and fourth moments of the experimental line shape can be compared with second and fourth moments calculated for the suggested structure. The second and fourth moments of the experimental line shape were determined by fitting the experimental FID curve with a polynomial of the form<sup>20</sup>

$$Q(t) = 1 - \frac{M_2}{2!}t^2 + \frac{M_4}{4!}t^4 - \frac{M_6}{6!}t^6 + \frac{M_8}{8!}t^8 \dots \quad (2)$$

The result of the fit leads to a second moment,  $(M_2)^{1/2} = 4.42 \pm 0.13$  G, and a fourth moment,  $(M_4)^{1/4} = 5.39 \pm 0.21$  G. The procedure for obtaining these numbers requires some elaboration at this point. The accuracy and precision of moments obtained from least-square fit of this type depend critically on the receiver dead time, and are sensitive to the truncation point of the data and the order of polynomial fitted. By changing these variables

one can determine the sensitivity of the results to these variables and their values, and the above numbers quoted for the second and fourth moments were obtained from averaging values from various fits up to the  $t^8$  term in  $Q(t)$ , with dead time of either 2.5 or 3.0  $\mu$ sec. The error limit covers the range of the values found. These errors are small because of the large signal-to-noise ratio of the experimental data and the short dead time of the spectrometer; however, it is probably better to consider them to be estimates of precision rather than accuracy since no primary calibration is available.

Using the reported structure of the sample,<sup>7</sup> theoretical second and fourth moments were calculated by the following equations appropriate for spin- $\frac{1}{2}$  nuclei in a polycrystalline sample:

$$M_2 = \frac{9}{20} \gamma^4 \hbar^2 \frac{1}{n} \sum_{n,k} \frac{1}{r_{nk}^6}, \quad (3)$$

$$M_4 = \frac{\gamma^8 \hbar^4}{n} \frac{27}{560} \left[ 9 \sum_{n,k} \left( \frac{1}{r_{nk}} \right)^{12} + \frac{23}{4} \sum_{n,k,l} \frac{1}{r_{nk}^6 r_{nl}^6} (2 - \cos^2 \phi_{knl} + \cos^4 \phi_{knl}) - \frac{1}{2} \sum_{n,k,l} \frac{1}{r_{nk}^6 r_{kl}^6} (2 - \cos^2 \phi_{nkl} + 3 \cos^4 \phi_{nkl}) \right. \\ \left. + 4 \sum_{n,k,l} \frac{1}{r_{nk}^6 r_{nl}^6 r_{kl}^6} (\cos^2 \phi_{kln} - \cos^2 \phi_{knl} - \cos^2 \phi_{nkl} + 3 \cos^2 \phi_{knl} \cos^2 \phi_{nkl}) \right. \\ \left. - \sum_{n,k,l} \frac{1}{r_{kl}^6 r_{nk}^6 r_{nl}^6} (\cos^2 \phi_{kml} - \cos^2 \phi_{nlk} - \cos^2 \phi_{nkl} + 3 \cos^2 \phi_{nlk} \cos^2 \phi_{nkl}) \right]. \quad (4)$$

$n, k, l$  are indices for spins.  $n=1$  if all locations are equivalent.  $\sum^*$  is a summation over indices  $n, k, l$  but omitting terms  $n=1$ ,  $n=k$ , and  $k=n$ . Equation (4) for the fourth moment can be derived from Van Vleck's formula<sup>21</sup> by properly averaging over all solid angles. The calculation for the suggested structure<sup>7</sup> of Th<sub>4</sub>H<sub>15</sub> leads to a second moment  $(M_2)^{1/2}$  of 4.48 G and a fourth moment  $(M_4)^{1/4}$  of 5.47 G. In the calculation of the second moment all protons within a radius of 12.5 Å were involved, while only 60 protons were involved in the calculation of the fourth moment. The agreement between the theoretical and experimentally determined moments furnishes confirmation for the structure suggested from the x-ray results. The non-Gaussian line shape is indicated by the ratio  $(M_4)^{1/4}/(M_2)^{1/2}$ . For a Gaussian line this ratio is 1.32, but for Th<sub>4</sub>H<sub>15</sub> it is only 1.22. Another way to fit the FID signal is by using an empirical function of the form,  $\exp(\frac{1}{2} - a^2 t^2)(\sin bt)/bt$ , which has been shown to fit the <sup>19</sup>F FID signal of CaF<sub>2</sub> single crystal with considerable success.<sup>22</sup> It is easily shown<sup>22</sup> that the second and fourth moments of such a function are  $M_2 = a^2 + \frac{1}{3}b^2$  and  $M_4 = 3a^4 + 2a^2b^2 + \frac{1}{5}b^4$ . By using the  $M_2$  and  $M_4$  calculated for the Th<sub>4</sub>H<sub>15</sub> proposed structure,<sup>7</sup> one obtains values of

$a$  and  $b$  and can generate the curve shown in Fig. 1. This curve is seen to fit the experimental FID signal well even to long times, and is still accurate at the second zero crossing point.

#### B. Relaxation analysis of motional properties

To extract information on the motion of protons from NMR measurements, one can use the following approximate equations appropriate for the various NMR relaxation times measured in this work.<sup>23-25</sup>

$$1/T_2 \approx \gamma^2 M_2 \tau \quad \text{for } \tau M_2^{1/2} \ll 1, \quad (5)$$

$$1/T_1 \approx \frac{4}{3} \gamma^2 M_2 (1/\omega_0^2 \tau) \quad \text{for } \omega_0 \tau \gg 1, \quad (6)$$

$$1/T_{1r} \approx \gamma^2 M_2 \tau / (1 + 4\omega_1^2 \tau^2), \quad (7)$$

where  $\omega_0$  is the Larmor frequency corresponding to external  $H_0$  field,  $\omega_1$  is the Larmor frequency corresponding to rf locking  $H_1$  field, and  $\tau$  is the correlation time for proton motion. These equations are derived from a single correlation time model for the proton motion, and if one further assumes that  $\tau$  obeys an Arrhenius relation, the corresponding activation energies  $\Delta E$  can be obtained from the temperature dependence of the relaxation parameters.

### C. Motional data from the $\text{Th}_4\text{H}_{15}$ sample A

The relaxation results for sample A are summarized in Fig. 2. Line-shape measurements indicate that motional narrowing starts at around 60 °C, and by 110 °C, the lines appear completely Lorentzian. The activation energy obtained from  $T_2$  above 120 °C is  $16.3 \pm 1.2$  kcal/mole.

The observed  $T_1$  can have two contributions:  $1/T_1 = 1/T_{1e} + 1/T_{1d}$ .  $T_{1e}$  is due to relaxation effects caused by conduction electrons, and  $T_{1d}$  is due to dipolar relaxation effect caused by the motion of nuclear spins. At temperatures below 110 °C, the conduction-electron effect appears to dominate  $T_1$  since a plot of  $T_1$  vs  $1/T$  can be fit with a straight line passing through the origin, as is illustrated in Fig. 3. This is the form of the relationship expected between  $T_1$  and  $1/T$  if the relaxation time is controlled by interaction with conduction-band electrons,<sup>26</sup> and differs qualitatively with behavior expected when lattice motions control  $T_1$ .<sup>26</sup> The slope of the line placed through the data points in Fig. 3 gives a value for the product  $T_1 T$  of  $180 \pm 10$  °Ksec, which differs from a value of 120 °K

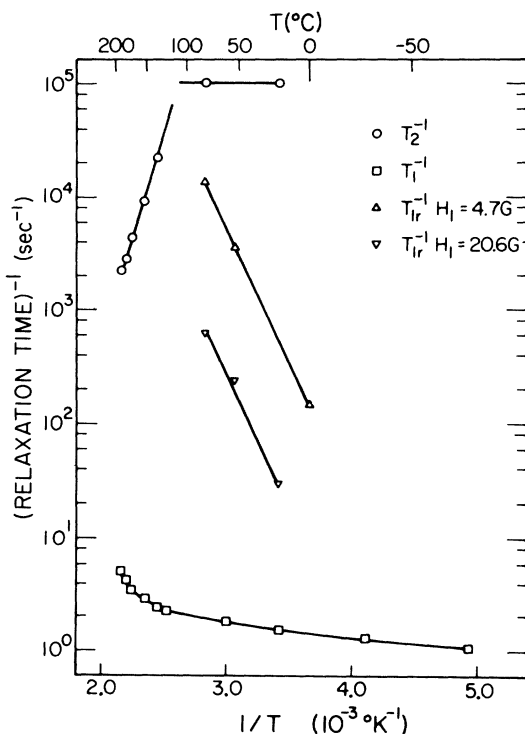


FIG. 2. Log of the inverse of the spin-spin relaxation time ( $T_2^{-1}$ ), spin-lattice relaxation time ( $T_1^{-1}$ ), and spin-lattice relaxation time in the rotating frame ( $T_{1r}^{-1}$ ) as a function of inverse temperature for sample A. Activation energies obtained from these data are  $16.3 \pm 1.2$ ,  $18.0 \pm 3.0$ , and  $10.9 \pm 0.7$  kcal/mole, respectively. The measuring frequency is 56.4 MHz.

sec obtained in previous work.<sup>11</sup> Using  $T_1 T = 180$  °Ksec and the usual expression for the  $T_1$  relaxation due to conduction electrons<sup>26</sup>

$$1/T_{1e} = \frac{64}{9} \pi^3 \hbar^{-3} \gamma_e^2 \gamma_n^2 \langle |\psi(0)|^2 \rangle E_F^2 [\rho(E_F)]^2 kT,$$

one can estimate the value of the quantity  $\xi$  defined as

$$\xi = \frac{\langle |\psi(0)|^2 \rangle_{E_F}}{\langle |\psi(0)|^2 \rangle_{\text{atom}}},$$

where  $\langle |\psi(0)|^2 \rangle_{\text{atom}}$  is the electron density at the proton site for a free hydrogen atom  $\langle |\psi(0)|^2 \rangle_{E_F}$ , the corresponding contribution from conduction electrons in  $\text{Th}_4\text{H}_{15}$  (an average over all orbits at the top of the Fermi distribution).  $\xi$  is a measure of conduction-band electron density near the proton. Making the same approximations as those in Ref. 11, one obtains  $0.1 \leq \xi \leq 0.5$ , which is somewhat smaller than the result reported in Ref. 11 using  $T_1 T = 120$  °Ksec, but confirms the fact that a significant portion of the hydrogen electrons are in the conduction band of  $\text{Th}_4\text{H}_{15}$ .

At higher temperatures the relaxation due to the proton motion becomes dominant, and by subtracting out the conduction-electron contribution, one obtains an activation energy for proton motion of  $18.0 \pm 3.0$  kcal/mole, in good agreement with the activation energy from the  $T_2$  data.

Two sets of  $T_{1r}$  data were obtained at substantially different holding fields,  $H_1 = 4.7$  G and  $H_1 = 20.6$  G, and are plotted in Fig. 2. The measured  $T_{1r}$ 's

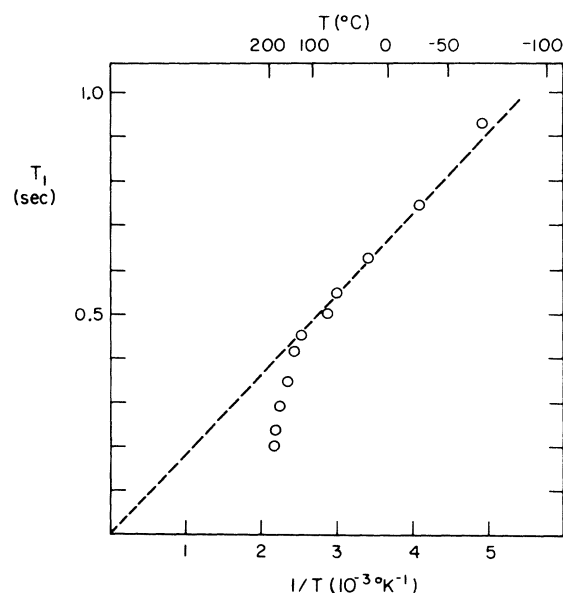


FIG. 3. Spin-lattice relaxation time ( $T_1$ ) as a function of inverse temperature for the sample A. The slope of the dashed line furnishes a value for the product  $T_1 T$  of  $180 \pm 10$  Ksec.

are proportional to  $H_1^2$  at a fixed temperature over the temperature range studied, and this is what the model for proton motion discussed above<sup>25</sup> would predict and is strong evidence that  $T_{1r}$  is dominated by lattice motion. Activation energies for proton motion of  $10.9 \pm 0.7$  kcal/mol are obtained from the slopes of the lines fitted through both sets of  $T_{1r}$  data. The difference between the activation energies for proton motion ( $16.3 \pm 1.2$  and  $18.0 \pm 3.0$  kcal/mole above  $120^\circ\text{C}$  and  $10.9 \pm 0.7$  kcal/mole below  $80^\circ\text{C}$ ) obtained from the NMR relaxation rates is well outside the limits of experimental error and suggest a more complex mechanism for proton motion than a simple single correlation time-activated process and could imply more than a single mechanism for proton motion.

In addition to activation energies, Eq. (5)–(7) can be used to obtain estimates of the correlation time  $\tau$  for the proton motion, and these results are illustrated in Fig. 4. One notes, however, that unlike the determination of activation energies, estimation of correlation times is dependent upon the numerical values for constants relating the relaxation times ( $T_1, T_2, T_{1r}$ ) to the correlation

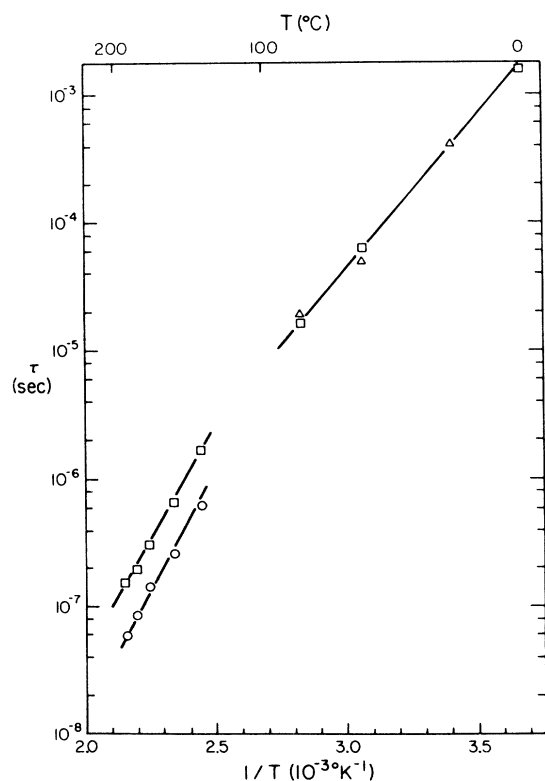


FIG. 4. Estimated correlation times  $\tau$  for proton motion as a function of inverse temperature in Th<sub>4</sub>H<sub>15</sub>: □ indicates  $\tau$ 's estimated from  $T_2$  data; ○, from  $T_1$  data; △, from  $T_{1r}$  with  $H_1 = 20.6$  G; and □ from  $T_{1r}$  with  $H_1 = 4.7$  G below  $100^\circ\text{C}$ .

time  $\tau$  in Eqs. (5)–(7). The nature of the theory and motional models usable in the development of Eqs. (5)–(7) is such that these constants are only defined within factors of two or three, and one must consider the correlation times obtained from their use as only order-of-magnitude estimates. As shown in Fig. 4, the  $\tau$ 's obtained from  $T_2$  data by using Eq. (5) are approximately 2.6 times the  $\tau$ 's from the  $T_1$  data using Eq. (6). Using Eq. (7), the  $\tau$ 's derived from  $T_{1r}$  data at different  $H_1$  holding fields agree with one another. Furthermore, both curves of  $\tau$ 's (i.e., above  $120^\circ\text{C}$  and below  $80^\circ\text{C}$ ) extrapolate to the same region in the intermediate temperature range, indicating that the available data coupled with Eqs. (5)–(7) give a rather consistent picture of the proton motion in the Th<sub>4</sub>H<sub>15</sub> sample.

Additional evidence for the applicability of the above interpretation of the data is obtained by using Eq. (7) to predict values of  $1/(T_{1r})_{\text{min}}$ . These are  $2.8 \times 10^4$  and  $6.4 \times 10^3 \text{ sec}^{-1}$  for  $H_1 = 4.7$  and  $20.6$  G, respectively, and are consistent with the available  $T_{1r}$  and  $T_2$  data in Fig. 3. The motional properties reported here differ significantly from previous measurements: the activation energy obtained for a temperature above  $120^\circ\text{C}$  is two to three times the values obtained in Ref. 10; motion narrowing of the line shape occurs at significantly higher temperature than that in Ref. 9.

#### D. Motional data from Th<sub>4</sub>H<sub>15</sub> sample B

Little difference was found between the NMR results on samples A and B at either room temperature or as the temperature was raised, although the  $T_1$  for sample B was 10% shorter than that for sample A. After maintaining the samples at temperatures near  $200^\circ\text{C}$  for an hour, a major difference was noted upon cooling, with sample B exhibiting a marked time-temperature hysteresis of all of the measured NMR properties, while sample A gave no indications of an effect in any of the NMR parameters measured. A more dramatic manifestation of this is that after the sample was cooled to room temperature, the proton motion took weeks to return to the original state, as indicated by the  $T_2$ ,  $T_1$ , and  $T_{1r}$  data (see Fig. 5). After the phenomena were observed the first time, the experiment was repeated a month later and the same effect was observed in  $T_1$ ,  $T_2$ , and  $T_{1r}$  measurements.

$T_1$  is dominated at room temperature by conduction-electron effects while  $T_2$  and  $T_{1r}$  are controlled by motional properties of the protons. The large time-temperature hysteresis observed in all of these parameters is strongly indicative of a phase change in the material on heating. The hys-

teresis is sufficiently large to be difficult to understand without the necessity of moving the thorium atoms to new locations since the mobility of the protons is such that they would relocate in times short compared to these, and the  $T_1$  results suggest that a change in band structure may be associated with the hysteresis. The fact that samples of the same composition and physical characteristics can behave so differently under mild heating is indicative that much still must be learned about this complex material, and detailed x-ray studies as a function of sample preparation and temperature are being conducted by Satterthwaite's research group at this time.

#### E. Multiple-pulse measurements

Multiple pulse measurements were performed on both samples *A* and *B* at 20 and  $-80^\circ\text{C}$ , and when no differences were noted, lower temperature measurements were performed only on sample *A*. Multiple pulse spectra for sample *A* are illustrated in Fig. 6 together with the eight-pulse spectrum of the reference used for the low-temperature measurements  $\text{Ca}(\text{OH})_2$ . It is noted that the line shapes observed are quite broad, and that the line center is a function of temperature.

First, the line shape will be discussed. It can be separated<sup>16,17</sup> into contributions from the second-order dipolar Hamiltonian,<sup>15</sup> magnetic field

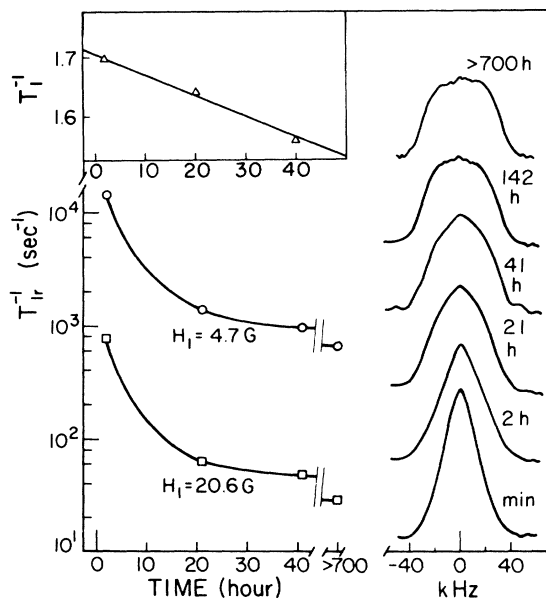


FIG. 5. Log of the inverse of the spin-lattice relaxation time ( $T_1^{-1}$ ), the spin-lattice relaxation time in the rotating frame ( $T_{1r}^{-1}$ ), and the line shape as a function of time for sample *B* after the sample was heated to  $460^\circ\text{K}$  and brought back to room temperature.

inhomogeneities, and a relaxation term. As discussed in the second section of this paper, this is experimentally done by performing a series of three multiple pulse experiments. Figure 6 shows the line shapes obtained from the conventional eight-pulse sequence, and Fig. 7 compares the decay times for the conventional eight-pulse measurements with the  $P_x - M_y$  phase-altered version at several different temperatures. The  $P_x - M_y$  phase-altered version is, as discussed earlier, primarily a measure of the relaxation contribution to the line shape, and Fig. 7 demonstrates that this term does not contribute significantly to the line shape below room temperature, but as the temperature is increased, it grows rapidly and dominates the multiple pulse line shape at  $80^\circ\text{C}$ . Spin lattice relaxation in the presence of the multiple pulse sequences has been discussed,<sup>27,28</sup> and the conclusion drawn that such relaxation could be qualitatively similar to a  $T_{1r}$ . That this is the case here can be seen by comparing the effective  $T_2$ 's under the  $P_x - M_y$  phase-altered eight-pulse sequence with the  $T_{1r}$ 's reported in Fig. 2. The major portion of the spherical density function for lattice motions contributing to relaxation under the influence of the multiple-pulse sequence used

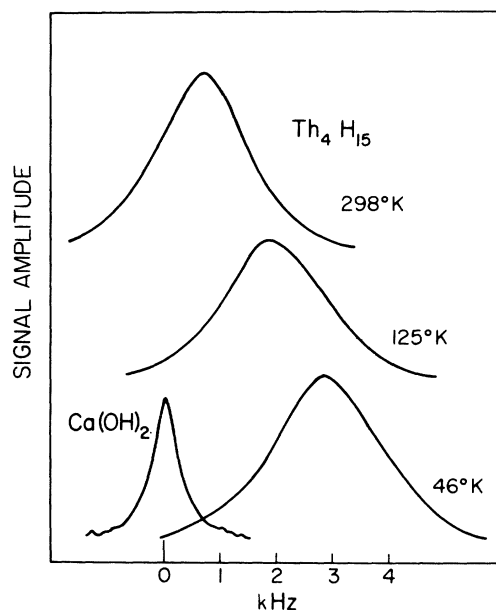


FIG. 6. Eight-pulse line shape and the peak locations of the  $\text{Th}_4\text{H}_{15}$  (sample-*A*) powder sample as a function of temperature using a  $\text{Ca}(\text{OH})_2$  single crystal as reference. The reference is oriented such that the major principal axis of the proton chemical shift tensor is parallel to the external magnetic field. A shift to the left in the figure signifies an increase in the value of  $\sigma$  [i.e., the internal magnetic field at the proton site is larger in  $\text{Th}_4\text{H}_{15}$  than  $\text{Ca}(\text{OH})_2$ ].

here should fall between the frequencies which contribute to the  $T_{1r}$ 's for the two locking fields used, 4.7 and 20.6 G, and, in fact, the effective  $T_2$ 's under the  $P_x - M_y$  sequence fall between the  $T_{1r}$  values at each temperature. Over the temperature range of the  $T_{1r}$  data, the multiple pulse results give an activation energy consistent with that obtained from the  $T_{1r}$  data. Thus, the relaxation contribution: (i) dominates the conventional eight-pulse line shape at 80 °C, (ii) can account for the increase observed in the conventional eight-pulse linewidth between room temperature and 80 °C (illustrated in Fig. 7), and (iii) appears to be an insignificant contribution below room temperature.

In order to determine what portion of the remainder of multiple-pulse line shape could be attributed to static magnetic field inhomogeneities, the  $-M_x$  version of the phase-altered eight-pulse experiment was performed. The effective  $T_2$ 's observed from the  $-M_x$  measurement were similar to the results of the conventional eight-pulse measurement over the range of temperatures investigated, thus indicating that almost all of the portion of the conventional eight-pulse line shape that is not due to relaxation effects can be attributed to the second-order dipolar Hamiltonian.

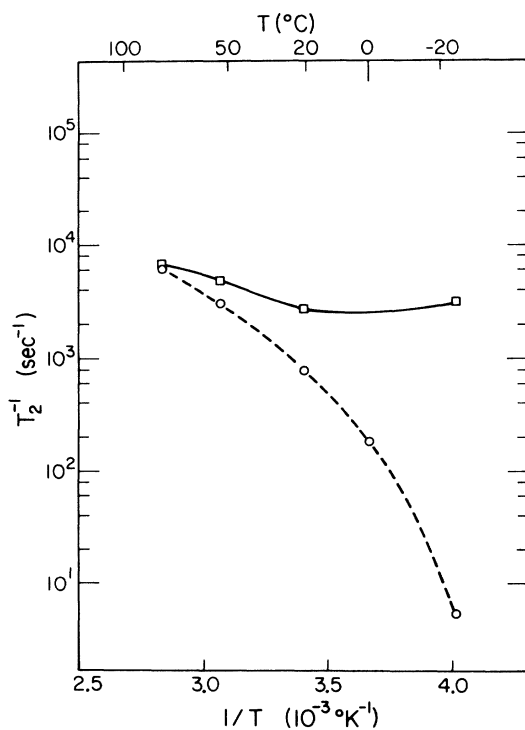


FIG. 7. Log of the inverse of the  $1/e$  decay points of the signal envelopes of the eight-pulse ( $\square$ ) and the  $P_x - M_y$  phase-altered eight-pulse ( $\circ$ ) sequences as a function of inverse temperature for the  $\text{Th}_4\text{H}_{15}$  powder sample.

The maximum possible field inhomogeneity Hamiltonian is estimated to be less than 16 ppm by this means, and this indicates that the combination of  $H_0$  inhomogeneity, field distortions caused by susceptibility effects, and chemical and Knight shift anisotropies do not add up to more than this value.

That the line shape is controlled by the second-order dipolar contribution at room temperature and below is not unexpected in this material with its very high proton concentration and consequently large proton-proton dipolar interaction. A  $T_2$  near 10  $\mu\text{sec}$  is observed and the cycle time of the eight-pulse sequence, 42  $\mu\text{sec}$ , is not rapid enough to keep the second-order dipolar term small. A separate check on the conclusion that the low-temperature line shape is primarily due to second-order dipolar effects was obtained by observing a rapid increase in the linewidth as the cycle time was lengthened.

While the field inhomogeneity Hamiltonian has been found to be small, the line center is observed to move by approximately 50 ppm as the temperature is lowered from room temperature to 46 °K. This is illustrated in Figs. 6 and 8. The observed shift was corrected<sup>29</sup> (reduced by up to 20%) for the measured<sup>30</sup> temperature-dependent bulk susceptibility (demagnetization effect) of the sample before constructing Figs. 6 and 8, and consequently, the experimentally observed shift was larger than that indicated in these figures. It should also be mentioned that the shift measured in this work is in the opposite direction to that reported in Ref. 9.

The absolute chemical shifts of protons in diamagnetic solids are typically of the order near

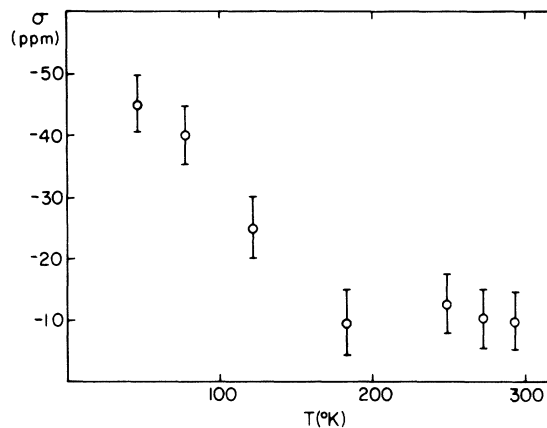


FIG. 8. Shift of the proton resonance line in  $\text{Th}_4\text{H}_{15}$  sample -A powder as a function of temperature. The results are reported relative to  $\text{Ca}(\text{OH})_2$  and have been corrected for the temperature-dependent susceptibility of  $\text{Th}_4\text{H}_{15}$ .

30 ppm,<sup>31</sup> and the Knight shift due to conduction electrons through the contact interaction is estimated to be  $-31.2$  ppm, using the experimental  $T_1T$  value of 180 Ksec and the Korringa relation<sup>32</sup>

$$T_1 \left( \frac{\Delta H}{H} \right)^2 = (\hbar/4\pi kT) \gamma_e^2 / \gamma_n^2.$$

Both of these contributions are temperature independent and are smaller than the temperature-dependent shift observed experimentally. Temperature-dependent shifts have been reported in rare-earth intermetallic compounds<sup>33</sup> and attributed to hyperfine couplings with the rare-earth electron spin. Additionally, the magnitude of temperature-dependent shifts found in several compounds with the A-15 structure (i.e., <sup>51</sup>V and <sup>69,71</sup>Ga in V<sub>3</sub>Ga<sup>34</sup>) has been correlated with the superconducting transition temperature of these materials, and an explanation has been suggested<sup>35</sup> based on the neces-

sity of a sharp peak in the electron density of states at the Fermi level. The temperature-dependent shift reported here for protons in Th<sub>4</sub>H<sub>15</sub> is large when compared to the expected size of the proton chemical or temperature-independent Knight shift and much smaller than the temperature-dependent shifts seen on other nuclei.<sup>34</sup>

#### ACKNOWLEDGMENTS

We wish to acknowledge several enlightening conversations with Professor I. J. Lowe of the University of Pittsburgh. The NMR studies of K.-F. Lau and R. W. Vaughan were supported by the Energy and Research and Development Administration Materials Science Program and by NAS-7-100, while sample preparation and characterization efforts of C. B. Satterthwaite received support from the NSF, DMR 7203010.

<sup>1</sup>W. M. Mueller, J. P. Blackledge, and G. G. Libowitz, *Metal Hydrides* (Academic, New York, 1968).

<sup>2</sup>N. W. Ashcroft, *Phys. Rev. Lett.* **21**, 1748 (1968).

<sup>3</sup>C. B. Satterthwaite and I. J. Toepke, *Phys. Rev. Lett.* **25**, 741 (1970).

<sup>4</sup>B. Stritzker and W. Buckel, *Z. Phys.* **257**, 1 (1972).

<sup>5</sup>T. Skoskiewicz, *Phys. Status Solidi* **11K**, 123 (1972).

<sup>6</sup>J. F. Miller, R. Caton, and C. B. Satterthwaite, *Phys. Rev. B* **14**, 2795 (1976).

<sup>7</sup>W. H. Zachariasen, *Acta Crystallogr.* **6**, 393 (1953); R. A. Beyerlein, M. H. Mueller, T. O. Brun, C. B. Satterthwaite, and R. Caton, *Bull. Am. Phys. Soc.* **20**, 422 (1975); J. M. Carpenter, M. H. Mueller, R. A. Beyerlein, T. G. Worlton, J. D. Jorgensen, T. O. Brun, K. Skold, C. A. Pelizzari, S. W. Peterson, N. Watonabe, M. Kimura, and J. E. Gunning, *Proceedings of the Neutron Diffraction Conference, Petten, Netherlands, 1975* (unpublished).

<sup>8</sup>H.-G. Schmidt and G. Wolf, *Solid State Commun.* **16**, 1085 (1975).

<sup>9</sup>W. Spalhoff, *Z. Phys. Chem. Neue Folge* **29**, 258 (1961).

<sup>10</sup>J. D. Will and R. G. Barnes, *J. Less Common Metals* **13**, 131 (1967).

<sup>11</sup>D. S. Schreiber, *Solid State Commun.* **14**, 177 (1974).

<sup>12</sup>R. Caton and C. B. Satterthwaite (unpublished).

<sup>13</sup>R. W. Vaughan, D. D. Elleman, L. M. Stacey, W.-K. Rhim, and J. W. Lee, *Rev. Sci. Instrum.* **43**, 1356 (1973).

<sup>14</sup>W.-K. Rhim, D. D. Elleman, and R. W. Vaughan, *J. Chem. Phys.* **58**, 1772 (1973); **59**, 3740 (1974).

<sup>15</sup>W.-K. Rhim, D. D. Elleman, L. B. Schreiber, and R. W. Vaughan, *J. Chem. Phys.* **60**, 4595 (1974); see also M. Mehring, *NMR Basic Principles and Progress*, edited by P. Diehl, E. Fluck, and R. Kosfeld (Springer-Verlag, Heidelberg, 1976), Vol. 11, p. 99.

<sup>16</sup>K.-F. Lau and R. W. Vaughan (unpublished).

<sup>17</sup>C. R. Dybowski and R. W. Vaughan, *Macromolecules* **8**, 50 (1975).

<sup>18</sup>For detailed description of the liquid transfer Helix-Tran refrigerator, see operating manual (Air Product and Chemicals, Inc., Allentown, Pa.).

<sup>19</sup>L. B. Schreiber and R. W. Vaughan, *Chem. Phys. Lett.* **28**, 586 (1974).

<sup>20</sup>I. J. Lowe and R. E. Norberg, *Phys. Rev.* **107**, 46 (1957).

<sup>21</sup>J. H. Van Vleck, *Phys. Rev.* **74**, 1168 (1948).

<sup>22</sup>A. Abragam, *The Principle of Nuclear Magnetic Resonance* (Oxford U.P., London, 1961), Chap. 4.

<sup>23</sup>N. Bloembergen, E. M. Purcell, and R. V. Pound, *Phys. Rev.* **73**, 679 (1948).

<sup>24</sup>D. E. Barnaal, M. Kopp, and I. J. Lowe, *J. Chem. Phys.* (to be published).

<sup>25</sup>D. C. Look and I. J. Lowe, *J. Chem. Phys.* **44**, 2995 (1966).

<sup>26</sup>Reference 22, Chap. 9.

<sup>27</sup>U. Haeblerlen and J. S. Waugh, *Phys. Rev.* **185**, 420 (1969).

<sup>28</sup>H. Schmiedel, D. Freude, and W. Grunder, *Phys. Lett.* **34**, 162 (1971); R. Muller and R. Willsch, *J. Mag. Reson.* **21**, 135 (1974); W. Grunder, *Wiss. Z.* **23**, 466 (1974).

<sup>29</sup>The observed shift was corrected for bulk susceptibility effects by treating both the sample and the reference as long cylinders; thus,

$$\delta = \delta_{\text{obs}} + \frac{1}{3}(2\pi)(\chi_{\text{v ref}} - \chi_{\text{v}}),$$

where  $\chi_{\text{v}}$  is the volume magnetic susceptibility. For Ca(OH)<sub>2</sub>,  $\chi_{\text{v}} = -0.665 \times 10^{-6}$  and for Th<sub>4</sub>H<sub>15</sub> the susceptibility is paramagnetic and dependent on temperature (30) ( $\chi_{\text{v}} \cong +0.93 \times 10^{-6}$  at 12°K and  $+0.57 \times 10^{-6}$  at 273°K, with the assumption that the density of the powder sample is 4.14 g/cm<sup>3</sup>, which is half the formula density of Th<sub>4</sub>H<sub>15</sub>). The corrected shift is thus presented in Figs. 6 and 8.

<sup>30</sup>Private communication of unpublished data, Jim Miller, Physics Dept., University of Illinois, Urbana, Ill.

- 61808.
- <sup>31</sup>K.-F. Lau and R. W. Vaughan, *Chem. Phys. Lett.* 33, 550 (1975).
- <sup>32</sup>J. Korringa, *Physica* 16, 601 (1950).
- <sup>33</sup>V. Jaccarino, B. T. Matthias, M. Peter, H. Suhl, and J. H. Wernick, *Phys. Rev. Lett.* 5, 251 (1960); see for a more recent review, E. D. Jones, *Phys. Rev.* 180, 455 (1969).
- <sup>34</sup>W. E. Blumberg, J. Eisinger, V. Jaccarino, and B. T. Matthias, *Phys. Rev. Lett.* 5, 149 (1960); see for a recent review, M. Weger and I. B. Goldberg, *Solid State Physics, Advances in Research and Applications*, edited by H. Ehrenreich, F. Seitz, and D. Turnbull (Academic, New York, 1973), Vol. 28.
- <sup>35</sup>A. M. Clogston and V. Jaccarino, *Phys. Rev.* 121, 1357 (1961).